

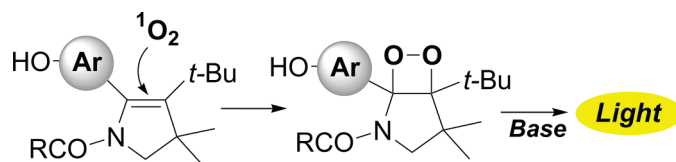
Synthesis of Thermally Stable Acylamino-Substituted Bicyclic Dioxetanes and Their Base-Induced Chemiluminescent Decomposition

Nobuko Watanabe, Yusuke Sano, Haruna Suzuki, Masatoshi Tanimura, Hisako K. Ijuin, and Masakatsu Matsumoto*

Department of Chemistry, Kanagawa University, Tsuchiya, Hiratsuka, Kanagawa 259-1293 Japan

matsumo-chem@kanagawa-u.ac.jp

Received June 20, 2010



Hydroxyaryl-substituted dioxetanes **2–4** fused with a pyrrolidine ring were selectively synthesized by singlet oxygenation of the corresponding dihydropyrroles **5–7**. These *N*-acylamino-substituted bicyclic dioxetanes were quite stable thermally, and **2a** and **2b** were estimated to possess half-lives of 32 and 34 y at 25 °C. When treated with TBAF (tetrabutylammonium fluoride) in DMSO, these dioxetanes underwent charge-transfer-induced decomposition (CTID) to emit yellow–orange light. The chemiluminescence efficiencies Φ^{CL} for dioxetanes **2** ranged from 10^{-6} to 10^{-2} . On the other hand, dioxetane **4** bearing a 4-(benzothiazol-2-yl)-3-hydroxyphenyl moiety showed chemiluminescent decomposition with high efficiency ($\Phi^{CL} = 0.15$) comparable to its oxy-analogue **26**. Prominent characteristics for CTID of the present dioxetanes were that the *N*-acylamino-group influenced the color of chemiluminescence as well as the rate of decomposition k^{CTID} , and furthermore an *N*-acyl substituent could decisively affect the singlet-chemiexcitation efficiency, as observed for the case of **2b**.

Introduction

An oxy-substituted dioxetane bearing a hydroxyaryl group provides one of the most versatile skeletons for the design and synthesis of high-performance chemiluminescence compounds, since the singlet oxygenation of a precursor enol ether

has been established as a reliable method for preparing a dioxetane with sufficient thermal stability.^{1–6} Another advantage is that such a dioxetane undergoes base-induced decomposition to give an excited aromatic ester, which is expected to emit light more effectively than a related aromatic ketone.^{7,8} An amino-substituted dioxetane should also be a promising entry to novel chemiluminescence compounds to give an

(1) For reviews of singlet oxygen, See: (a) Denny, R. W.; Nickon, A. Sensitized Photooxygenation of Olefins; In *Organic Reactions*; Wiley: New York, 1973; Vol. 20, pp 133–336. (b) Schaap, A. P.; Zaklica, K. A. In *Singlet Oxygen*; Wasserman, H. H., Murray, R. W., Eds.; Academic Press: New York, 1979; pp 173–242. (c) Baumstark, A. L. In *Singlet O₂*; Frimer, A. A., Ed.; CRC Press: Boca Raton, FL, 1985; Vol. 2, pp 1–35.

(2) For reviews of 1,2-dioxetane, see: (a) Bartlett, P. D.; Landis, M. E. In *Singlet Oxygen*; Wasserman, H. H., Murray, R. W., Eds.; Academic Press: New York, 1979; pp 243–286. (b) Adam, W. In *The Chemistry of Peroxide*; Patai, S., Ed.; Wiley: New York, 1983; pp 829–920. (c) Adam, W. In *Small Ring Heterocycles*; Hassner, A., Ed.; Wiley: New York, 1986; pp 351–429. (d) Adam, W.; Heil, M.; Mosandl, T.; Saha-Möller, C. R. In *Organic Peroxides*; Ando, W., Ed.; Wiley: New York, 1992; pp 221–254. (e) Saha-Möller, C. R.; Adam, W. In *Comprehensive Heterocyclic Chemistry II. A Review of the Literature 1982–1995*; Padwa, A., Ed.; Pergamon: New York, 1996; pp 1041–1082. (f) Adam, W.; Trofimov, A. V. In *The Chemistry of Peroxides*; Rappoport, Z., Ed.; Wiley: New York, 2006; Vol. 2, pp 1171–1209. (g) Baader, W. J.; Stevani, C. V.; Bastos, E. L. In *The Chemistry of Peroxides*; Rappoport, Z., Ed.; Wiley: New York, 2006; Vol. 2, pp 1211–1278.

(3) (a) Schaap, A. P.; Gagnon, S. D. *J. Am. Chem. Soc.* **1982**, *104*, 3504–3506. (b) Schaap, A. P.; Handley, R. S.; Giri, B. P. *Tetrahedron Lett.* **1987**, *28*, 935–938. (c) Schaap, A. P.; Chen, T. S.; Handley, R. S.; DeSilva, R.; Giri, B. P. *Tetrahedron Lett.* **1987**, *28*, 1155–1158.

(4) For reviews of dioxetane-based chemiluminescence, see: (a) Beck, S.; Köster, H. *Anal. Chem.* **1990**, *62*, 2258–2270. (b) Adam, W.; Reihardt, D.; Saha-Möller, C. R. *Analyst* **1996**, *121*, 1527–1531. (c) Matsumoto, M. *J. Photochem. Photobiol., C* **2004**, *5*, 27–53. (d) Matsumoto, M.; Watanabe, N. *Bull. Chem. Soc. Jpn.* **2005**, *78*, 1899–1920.

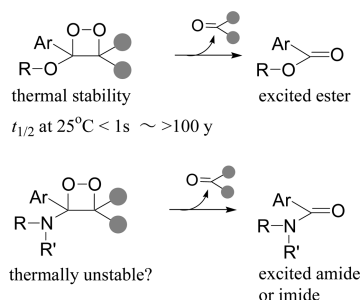
(5) Edwards, B.; Sparks, A.; Voyta, J. C.; Bronstein, I. In *Bioluminescence and Chemiluminescence, Fundamentals and Applied Aspects*; Campbell, A. K., Kricka, L. J., Stanley, P. E., Eds.; Wiley: Chichester, UK, 1994; pp 56–59.

(6) (a) Bronstein, I.; Edwards, B.; Voyta, J. C. *J. Biolumin. Chemilumin.* **1989**, *4*, 99–111. (b) Edwards, B.; Sparks, A.; Voyta, J. C.; Bronstein, I. *J. Biolumin. Chemilumin.* **1990**, *5*, 1–4. (c) Trofimov, A. V.; Vasil'ev, R. F.; Mielke, K.; Adam, W. *Photochem. Photobiol.* **1995**, *62*, 35–43. (d) Adam, W.; Bronstein, I.; Edwards, B.; Engel, T.; Reinhardt, D.; Schneider, F. W.; Trofimov, A. V.; Vasil'ev, R. F. *J. Am. Chem. Soc.* **1996**, *118*, 10400–10407. (e) Sabelle, S.; Renard, P.-Y.; Pecorella, K.; de Suzzoni-Déard, S.; Crémion, C.; Grassi, J.; Mioskowski, C. *J. Am. Chem. Soc.* **2002**, *124*, 4874–4880.

(7) An aromatic ketone generally causes a low-lying $n-\pi^*$ state, which results in a substantial decrease in fluorescence efficiency.⁸

(8) (a) Turro, N. J. *Modern Molecular Photochemistry of Organic Molecules*; University Science: Sausalito, CA, 2010; pp 230–234. (b) Valeur, B. *Molecular Fluorescence, Principles and Applications*; Wiley: New York, 2006; pp 57–58.

SCHEME 1. Oxy-Substituted Dioxetane and Amino-Substituted Dioxetane



amide or imide as an emitter (Scheme 1). However, little is known about amino-substituted dioxetanes that show sufficient thermal stability to permit handling at room temperature, though the 1,2-addition of singlet oxygen to enamine precursors, such as enecarbamates, readily takes place.^{1,2,9}

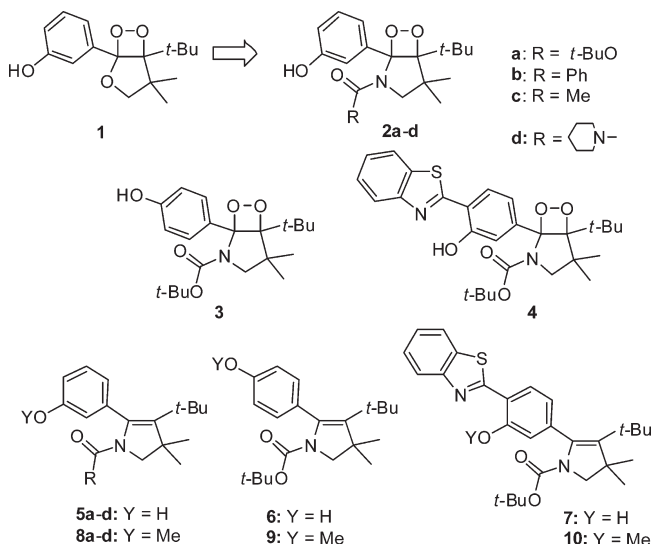
In the course of our investigation of high-performance chemiluminescence compounds, we attempted to realize thermally stable amino-substituted dioxetanes by modifying the skeleton of oxy-substituted bicyclic dioxetane **1**, which shows marked thermal stability.¹⁰ The thus-realized dioxetanes were 2-acyl-1-aryl-5-*tert*-butyl-4,4-dimethyl-2-aza-6,7-dioxabicyclo-[3.2.0]heptanes **2a–d**, **3**, and **4**.^{11,12} In addition to the synthesis of these dioxetanes, we report here that the base-induced decomposition of these *N*-acylamino-substituted dioxetanes showed unique chemiluminescence, the properties of which changed with an *N*-acyl substituent as well as with an aromatic moiety (Chart 1).

Results and Discussion

1. Synthesis of Acylamino-Substituted Bicyclic Dioxetanes.

Acylamino-substituted bicyclic dioxetanes **2a–d**, **3**, and **4** were prepared by singlet oxygenation of the corresponding *N*-acyl-5-aryl-4-*tert*-butyl-3,3-dimethyl-2,3-dihydropyrroles **5a–d**, **6**, and **7**. These precursors were synthesized through several steps starting from 1-(*N*-Boc)amino-2,2,4,4-tetramethylpentan-3-one **11** as illustrated in Scheme 2. (*N*-Boc)aminoketone **11** was obtained by oxidation of 1-(*N*-Boc)amino-2,2,4,4-tetramethylpentan-3-ol, which was synthesized from commercially available pivaloyl-acetonitrile by the introduction of two methyls followed by reduction with LiAlH₄. The first step in the synthetic sequences leading to **5a–d** was the *N*-substitution of **11** with 3-methoxybenzyl chloride **12** to give *N*-benzyl-*N*-(Boc)aminoketone **13**.

CHART 1. Acylamino-Substituted Dioxetanes **2**, **3**, and **4** and Their Precursors **5–10**



N-(Boc)benzylamines have been known to produce a benzylic anion by the action of a base such as LDA.¹³ Thus, we conducted the LDA-mediated intramolecular cyclization of **13** at 45 °C to give a stereoisomeric mixture of hydroxypyrrolidine **14a** (**14a-trans**:**14a-cis** = 2:3) in 94% yield. These stereoisomers could be isolated in pure form by column chromatography on SiO₂. The stereochemistry of **14a-trans** was determined by X-ray single crystallographic analysis: the ORTEP view of **14a-trans** is shown in the Supporting Information [Figure S1(a)].

The dehydration of alcohol **14a-trans** was achieved by the use of SOCl₂/pyridine in ether to give dihydropyrrole **8a** in quantitative yield, while **14a-cis** underwent dehydration sluggishly under similar conditions to give **8a** in only 30% yield. However, **14a-cis** could be effectively reused, since its retrocyclization took place to give **13** upon treatment with *t*-BuOK in *N*-methylpyrrolidone (NMP). Therefore, we decided to use a deprotected form of **14a-trans**, e.g., *N*-free pyrrolidine **15**, as a key intermediate to synthesize **8b–d**. Deprotection of *N*-Boc in **14a-trans** was carried out by catalysis with trifluoroacetic acid to give exclusively **15**. *N*-Acylation of **15** with benzoyl chloride, acetic anhydride, or piperidinocarbonyl chloride gave the corresponding *N*-acylpyrrolidines, **14b–d-trans**, in 75–90% yields. These hydroxypyrrolidines were smoothly dehydrated to the corresponding dihydropyrroles **8b–d** in 83–97% yields. Demethylation of a methoxyphenyl group in **8a–d** proceeded with sodium methylthioate in hot DMF to give the corresponding hydroxyphenyl-substituted dihydropyrroles **5a–d** in 73–99% yields.

Dihydropyrrole derivative **6** bearing a 4-hydroxyphenyl group was synthesized through **17**, **18**, and **9** according to the synthetic sequences from **12** to **5a** by the use of 4-methoxybenzyl chloride (**16**) instead of **12**. Synthesis of dihydropyrrole **7** bearing a 4-(benzothiazol-2-yl)-3-hydroxyphenyl moiety started from the *N*-substitution of **11** with benzothiazolyl-substituted benzyl chloride **19** to give aminoketone **20**. As in the case of **13**, aminoketone **20** was subjected to base-mediated cyclization to give **21**, which was followed by dehydration to **10** and subsequent demethylation to give **7**.

When *N*-(Boc)dihydropyrrole **5a** was irradiated together with a catalytic amount of tetraphenylporphyrin (TPP) in

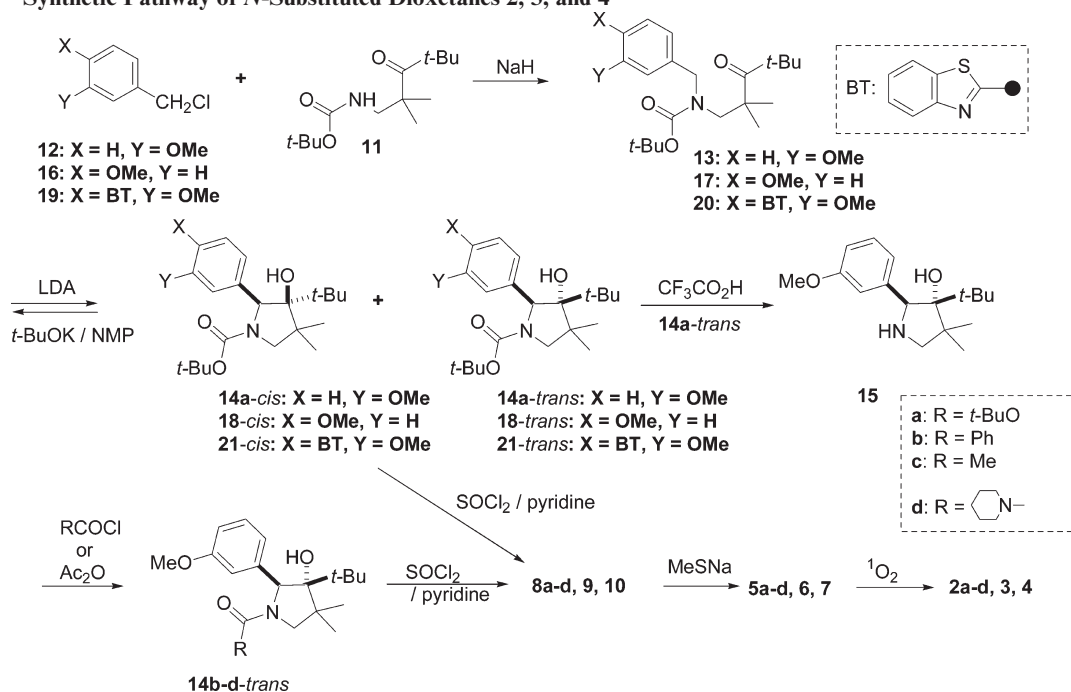
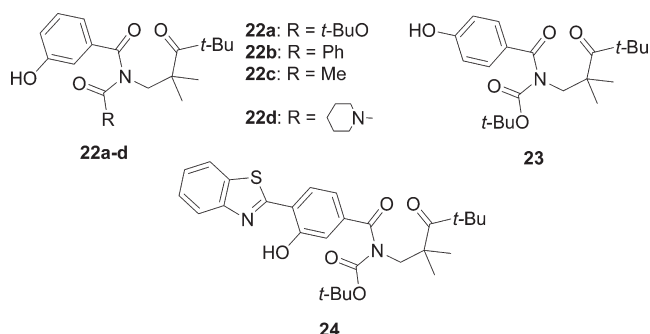
(9) (a) Adam, W.; Bosio, S. G.; Turro, N. J. *J. Am. Chem. Soc.* **2002**, *124*, 8814–8815. (b) Adam, W.; Bosio, S. G.; Turro, N. J. *J. Am. Chem. Soc.* **2002**, *124*, 14004–14005. (c) Poon, T.; Turro, N. J.; Chapman, J.; Lakshminarashimhan, J.; Lei, X.; Jockusch, S.; Franz, R.; Washington, I.; Adam, W.; Bosio, S. G. *Org. Lett.* **2003**, *5*, 4951–4953. (d) Adam, W.; Bosio, S. G.; Turro, N. J.; Wolff, B. T. *J. Org. Chem.* **2004**, *69*, 1704–1715.

(10) (a) Matsumoto, M.; Watanabe, N.; Kasuga, N. C.; Hamada, F.; Tadokoro, K. *Tetrahedron Lett.* **1997**, *38*, 2863–2866. (b) Adam, M.; Matsumoto, M.; Trofimov, A. V. *J. Org. Chem.* **2000**, *65*, 2078–2082. (c) Matsumoto, M.; Mizoguchi, Y.; Motoyama, T.; Watanabe, N. *Tetrahedron Lett.* **2001**, *42*, 8869–8872. (d) Matsumoto, M.; Akimoto, T.; Matsumoto, Y.; Watanabe, N. *Tetrahedron Lett.* **2005**, *46*, 6075–6078.

(11) A part of this work has been reported as a preliminary communication.¹²

(12) Matsumoto, M.; Sano, Y.; Watanabe, N.; Ijuin, H. K. *Chem. Lett.* **2006**, *35*, 882–883.

(13) (a) Park, Y. S.; Boys, M. L.; Beak, P. *J. Am. Chem. Soc.* **1996**, *118*, 3757–3758. (b) Faibish, N. C.; Park, Y. S.; Lee, S.; Beak, P. *J. Am. Chem. Soc.* **1997**, *119*, 11561–11570. (c) Kim, B. J.; Park, Y. S.; Beak, P. *J. Org. Chem.* **1999**, *64*, 1705–1708.

SCHEME 2. Synthetic Pathway of *N*-Substituted Dioxetanes 2, 3, and 4CHART 2. Keto Imides 22, 23, and 24 As a Product of Thermal Decomposition of *N*-Acylamino-Substituted Dioxetanes 2, 3, and 4

CH₂Cl₂ with a Na-lamp under an O₂ atmosphere at 0 °C, singlet oxygenation of **5a** proceeded smoothly to give dioxetane **2a** exclusively. Chromatographic purification of the photolysate gave pure **2a** in 97% yield. Dihydropyrrole analogues **5b–d**, **6**, and **7** were similarly dioxxygenated with singlet oxygen to afford the corresponding bicyclic dioxetanes **2b–d**, **3**, and **4** in isolated yields of 85–100%. The structure of these dioxetanes was determined by ¹H NMR, ¹³C NMR, IR, mass, HRMass spectral data, and elemental analyses. Among these dioxetanes, X-ray single crystallographic analysis was only attained for **4**, the ORTEP view of which is shown in the Supporting Information [Figure S1(b)].

All of these *N*-acyldioxetanes **2a–d**, **3**, and **4** were thermally stable enough to permit handling at room temperature, though they decomposed quantitatively into the corresponding keto imides **22a–d**, **23**, and **24** when heated in *p*-xylene (Chart 2). To determine the thermodynamic profiles for the thermolysis of these dioxetanes, we selected **2a** and **2b** as representative compounds and heated them individually at 90–110 °C in *p*-xylene-*d*₁₀. The time-courses monitored by ¹H NMR showed

that the thermolysis of these dioxetanes proceeded according to first-order kinetics. Thus, the following thermodynamic parameters were estimated from Eyring plots: $\Delta H^\ddagger/\text{kJ mol}^{-1}$, $\Delta S^\ddagger/\text{J K}^{-1} \text{mol}^{-1}$, and $\Delta G^\ddagger/\text{kJ mol}^{-1}$ were 124, −4.7, and 125 for **2a**, and 125, −0.5, and 125 for **2b**, respectively (Supporting Information, Figures S2 and S3). From these values, the half-lives (*t*_{1/2}) were estimated to be 32 y for **2a** and 34 y for **2b** at 25 °C. These results showed that the acylamino-substituted dioxetanes synthesized here belonged to a class of dioxetanes with high thermal stability.² The marked thermal stability of **2** is most likely attributed to the synergetic effect of a fused five-membered ring and a bulky *tert*-butyl group as a prop or wall¹⁴ to prevent twisting of the dioxetane ring: stretching of the O–O bond has been believed to cause decomposition of the dioxetane ring.^{2,15} The effect of an electron-withdrawing group on a nitrogen may also contribute to the stabilization of dioxetanes **2**.

Notably, dioxetanes **2a–d** and **4** displayed two groups of peaks due to conformational isomerism in ¹³C NMR and ¹H NMR spectra: isomeric ratios were 55:45 for **2a**, 50:50 for **2b** and **2c**, 76:24 for **2d**, and 52:48 for **4** in CDCl₃ at 25 °C. For these dioxetanes, two types of conformational isomerism can formally exist, as shown in Scheme 3, in which **2a** is shown as a representative compound. Type A isomerism occurs around the axis that joins Boc carbonyl to nitrogen to give rotamers **2a-antiacyl** and **2a-syn-acyl**, whereas the other type (type B) occurs around the axis that joins 3-methoxyphenyl

(14) (a) Watanabe, N.; Kikuchi, M.; Maniwa, Y.; Ijuin, H. K.; Matsumoto, M. *J. Org. Chem.* **2010**, *75*, 879–884. (b) Tanimura, M.; Watanabe, N.; Ijuin, H. K.; Matsumoto, M. *J. Org. Chem.* **2010**, *75*, 3678–3684.

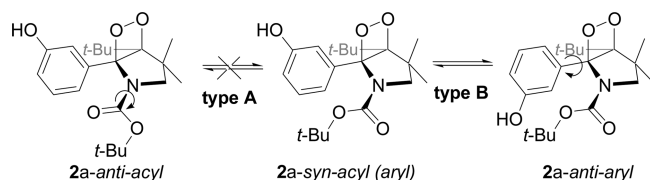
(15) (a) Dewar, M. J. S.; Kirschner, S. J. *Am. Chem. Soc.* **1974**, *96*, 7578–7589. (b) Turro, N. J.; Lechtken, P.; Shore, N. E.; Schuster, G.; Steinmetzer, H.-C.; Yekta, A. *Acc. Chem. Res.* **1974**, *7*, 97–105. (c) Adam, W.; Baader, W. J. *J. Am. Chem. Soc.* **1985**, *107*, 410–416. (d) Reguero, M.; Bernardi, F.; Bottoni, A.; Olivucci, M.; Robb, M. J. *Am. Chem. Soc.* **1991**, *113*, 1566–1572. (e) Wilson, T.; Halpern, A. M. *J. Phys. Org. Chem.* **1995**, *8*, 359–363. (f) Vasil'ev, R. F. *J. Biolumin. Chemilumin.* **1998**, *13*, 69–74. (g) Tanaka, C.; Tanaka, J. J. *Phys. Chem. A* **2000**, *104*, 2078–2090.

TABLE 1. TBAF-Induced Chemiluminescence of Acylamino-Substituted Bicyclic Dioxetanes **2a–d**, **3**, and **4**^a

| dioxetane | λ_{\max}/nm | $\Phi^{\text{CL } b}$ | Φ^{I} | Φ_{S} | $k^{\text{CTID}}_{\text{fast}}/\text{s}^{-1}$ | $k^{\text{CTID}}_{\text{slow}}/\text{s}^{-1}$ |
|------------------------|----------------------------|-----------------------|----------------------|-------------------|---|---|
| 2a | 571 | 8.5×10^{-3} | 3.9×10^{-2} | 0.22 | 0.70 | 4.0×10^{-2} |
| 2b | 600 | 3.4×10^{-6} | 2.0×10^{-3} | 0.0017 | 1.2 | 1.4×10^{-1} |
| 2c | 588 | 4.4×10^{-3} | 2.1×10^{-2} | 0.21 | 2.3 | 7.5×10^{-2} |
| 2d | 564 | 1.8×10^{-2} | 8.4×10^{-2} | 0.21 | 2.7×10^{-3} | |
| 3 | 471 | 1.1×10^{-7} | | | 0.14 | |
| 4 | 542 | 0.15 | 0.64 | 0.24 | 1.2×10^{-4} | |
| 1 ^c | 467 | 0.11 | 0.24^d | 0.46 | 2.8×10^{-2} | |
| 26 ^e | 492 | 0.28 | 0.66^f | 0.42 | 4.5×10^{-4} | |

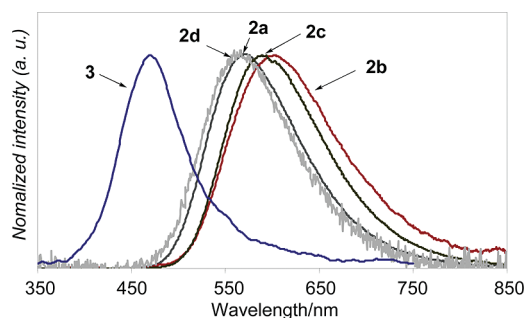
^aUnless otherwise stated, reactions were carried out in DMSO at 25 °C. ^b Φ^{CL} values were estimated based on the value reported for 3-adamantylidene-4-methoxy-4-(3-siloxyphenyl)-1,2-dioxetane.^{19,20} ^cReference 10c. Chemiluminescent decomposition was carried out in a TBAF/acetonitrile system. ^dReference 10b. ^eReference 14b. Chemiluminescent decomposition was carried out in a TBAF/acetonitrile system at 45 °C. ^fReference 10d.

SCHEME 3. Rotational Isomerism of *N*-Acylamino-Substituted Bicyclic Dioxetane **2a**



to a dioxetane carbon to afford rotamers **2a-antiaryl** and **2a-syn-aryl**. The fact that neither the ¹³C NMR nor ¹H NMR spectrum of 4-hydroxyphenyl-analogue **3** showed any evidence of *syn-anti* isomerism strongly suggests that the isomerism observed for **2a–d** and **4** was due to type B rotational isomerism. Such rotational isomerism appeared to readily occur at room temperature. Crystalline **4** used for X-ray single crystallographic analysis showed a ¹H NMR spectrum of a mixture of rotamers (52:48) when dissolved in CDCl₃ at room temperature.

2. Base-Induced Chemiluminescent Decomposition of Acylamino-Substituted Bicyclic Dioxetanes. A dioxetane bearing an oxidophenyl anion produced from a phenolic dioxetane such as **1** decomposes rapidly to give an aromatic ester accompanied by the emission of light by an intramolecular charge-transfer-induced decomposition (CTID) mechanism.^{4,16–18} Dioxetanes **2a–d** were also expected to undergo CTID to give a new type of emitter bearing an imide moiety **22a–d**,

FIGURE 1. Chemiluminescence spectra of dioxetanes **2a–d** and **3**.

respectively. When a solution of **2a** in DMSO was added to a large excess of tetrabutylammonium fluoride (TBAF) in DMSO, **2a** decomposed to give yellow light with maximum wavelength ($\lambda_{\max}^{\text{CL}}$) = 571 nm and chemiluminescence efficiency (Φ^{CL}) = 8.5×10^{-3} (Figure 1, Table 1).^{19,20} TBAF similarly induced the decomposition of **2b–d** to give green to yellow light, the spectra of which are shown in Figure 1. The chemiluminescence properties for **2a–d** are summarized together with those for **3** and **4**, and oxy-analogues **1** and **26** (vide infra). The results in Table 1 show that an *N*-acyl group considerably affected Φ^{CL} as well as $\lambda_{\max}^{\text{CL}}$ of **2**: while Φ^{CL} increased in the order **2b** \ll **2c** $<$ **2a** $<$ **2d**, $\lambda_{\max}^{\text{CL}}$ decreased in the order **2b** $>$ **2c** $>$ **2a** $>$ **2d**.

All of the freshly spent reaction mixtures of **2a–d** gave the corresponding imides **22a–d** in high yields after careful neutralization. Oxidophenyl anions **25a–d** generated from authentic **22a–d** in TBAF/DMSO showed fluorescence, the spectra of which coincided with those of the corresponding chemiluminescences from **2a–d**. Therefore, **25a–d** were undoubtedly the emitters produced from **2a–d**, respectively (Scheme 4). On the basis of their fluorescence efficiencies (Φ^{f}), chemiexcitation efficiencies ($\Phi_{\text{S}} = \Phi^{\text{CL}}/\Phi^{\text{f}}$) were estimated. As summarized in Table 1, Φ_{S} values were 0.21–0.22 for **2a**, **2c**, and **2d**, but only 0.0017 for **2b**. For **2b**, not only Φ_{S} but also Φ^{f} of the emitter were far smaller than those for **2a**, **2c**, and **2d**. The results show that an *N*-acyl substituent of **2** could significantly affect Φ_{S} as well as $\lambda_{\max}^{\text{CL}}$ and Φ^{f} . The π -electron system of an aromatic carbonyl spread over the imide moiety would change with the character of the *N*-acyl group for emitter **25**. Thus, we can imagine that both $\lambda_{\max}^{\text{CL}}$ and Φ^{f} would change with the structure of the emitter imide.

(16) The chemiluminescent (CL) decomposition of hydroxyphenyl-substituted dioxetanes has been proposed to proceed by a CIEEL⁹ (chemically initiated electron exchange luminescence) mechanism, where an initially formed radical ion pair annihilates by back electron transfer (BET) to afford an excited aromatic carbonyl compound. However, it is unclear whether such a CL reaction includes BET as a fundamental process. Therefore, we have recently been using the term CTID, which includes CIEEL and other CT-induced mechanisms.

(17) (a) Koo, J.-Y.; Schuster, G. B. *J. Am. Chem. Soc.* **1977**, *99*, 6107–6109. (b) Koo, J.-Y.; Schuster, G. B. *J. Am. Chem. Soc.* **1978**, *100*, 4496–4503. (c) Zaklika, K. A.; Kissel, T.; Thayer, A. L.; Burns, P. A.; Schaap, A. P. *Photochem. Photobiol.* **1979**, *30*, 35–44. (d) Catalani, L. H.; Wilson, T. *J. Am. Chem. Soc.* **1989**, *111*, 2633–2639. (e) McCapra, F. *J. Photochem. Photobiol., A* **1990**, *51*, 21–28. (f) McCapra, F. In *Chemiluminescence and Bioluminescence*; Hastings, J. W., Kricka, L. J., Stanley, P. E., Eds.; Wiley: New York, 1996; pp 7–15. (g) Adam, W.; Bronstein, I.; Trofimov, T.; Vasil'ev, R. F. *J. Am. Chem. Soc.* **1999**, *121*, 958–961. (h) Adam, W.; Matsumoto, M.; Trofimov, T. *J. Am. Chem. Soc.* **2000**, *122*, 8631–8634. (i) Nery, A. L. P.; Weiss, D.; Catalani, L. H.; Baader, W. *J. Tetrahedron* **2000**, *56*, 5317–5327.

(18) (a) Takano, Y.; Tsunesada, T.; Isobe, H.; Yoshioka, Y.; Yamaguchi, K.; Saito, I. *Bull. Chem. Soc. Jpn.* **1999**, *72*, 213–225. (b) Tanaka, J.; Tanaka, C.; Matsumoto, M. In *Bioluminescence and Chemiluminescence*; Tsuji, A., Matsumoto, M., Maeda, M., Kricka, L. J., Stanley, P. E., Eds.; World Scientific: Singapore, 2004; pp 205–208. (c) Tanaka, C.; Tanaka, J.; Matsumoto, M. In *Bioluminescence and Chemiluminescence*; Tsuji, A., Matsumoto, M., Maeda, M., Kricka, L. J., Stanley, P. E., Eds.; World Scientific: Singapore, 2004; pp 209–212. (d) Isobe, H.; Takano, Y.; Okumura, M.; Kuramitsu, S.; Yamaguchi, K. *J. Am. Chem. Soc.* **2005**, *127*, 8667–8679.

(19) Φ^{CL} was estimated based on the value 0.29 for the chemiluminescent decomposition of 3-adamantylidene-4-methoxy-4-(3-oxidophenyl)-1,2-dioxetane in an TBAF/DMSO system.²⁰

(20) Trofimov, A. V.; Mielke, K.; Vasil'ev, R. F.; Adam, W. *Photochem. Photobiol.* **1996**, *63*, 463–467.

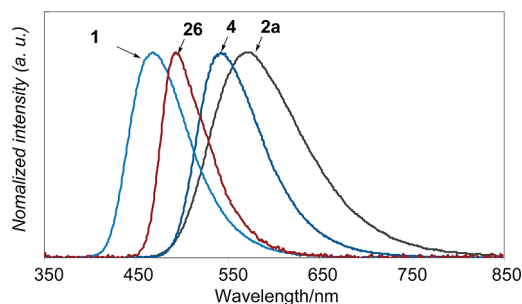


FIGURE 2. Comparison in chemiluminescence spectra between oxy-substituted dioxetanes **1** and **26** and *N*-(Boc)amino-substituted dioxetanes **2a** and **4**.

SCHEME 4. Base-Induced Chemiluminescence of *N*-Acylamino-Substituted Dioxetanes

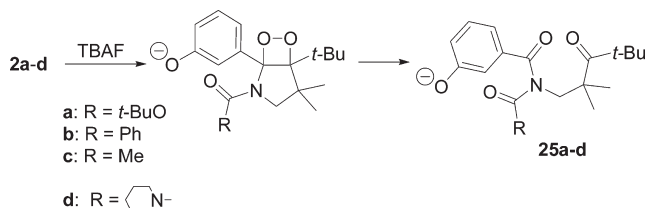
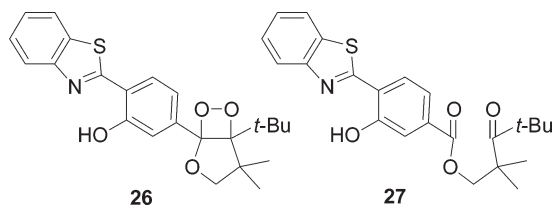


CHART 3. Oxy-Substituted Dioxetane **26 Bearing a Benzo-thiazolyl Group and Its Decomposition Product **27****



However, it is unclear why even Φ_S was significantly affected by an *N*-acyl group as observed for **2b**.

We finally examined the CTID of dioxetane **4** and compared its chemiluminescence properties with those for its oxy-analogue **26** as well as with those for **2a–d**: **26** has very recently been reported as an excellent chemiluminescence compound with high Φ_{CL} (Chart 3).^{14b} Upon treatment with a large excess of TBAF in DMSO at 25 °C, **4** decomposed to effectively emit yellow light (Figure 2) with properties summarized in Table 1, which also gives the chemiluminescence properties for **26**. We can see from Table 1 that Φ_{CL} of **4** was far higher than those of **2a–d** and was comparable to that of **26**. The high Φ_{CL} of **4** was due to high Φ^I as in the case of **26**: the Φ^I of the oxidoanion of **24** was measured to be 0.64, so that the chemiexcitation efficiency Φ_S of **4** was estimated to be 0.24 (Table 1). Another characteristic was that λ_{max}^{CL} for **4** was considerably shorter than that of parent **2a**, in contrast to the case of **26**, for which λ_{max}^{CL} was longer than that of parent **1**. Participation of *N*-Boc carbonyl to the π -electron system of **25a** and oxido anion of **24** presumably causes such a difference, different from the cases of **1** and **26**, for which emitters are aromatic esters. An MO calculation (B3LYP/6-31G(d)) supported this idea: energy gaps corresponding to $\pi^* \rightarrow \pi$ emission, ΔE , were estimated to be 3.01 eV for 2,2,4,4-tetramethyl-3-oxopentyl 3-oxidobenzoate, emitter from

parent **1**, 2.83 eV for oxido anion of **27**, while ΔE was 2.87 eV for **25a** and 2.81 eV for oxido anion of **24**.²¹

The time-course of CTID showed that **2a** underwent dual-phase decomposition, consisting of fast and slow reactions (Supporting Information, Figure S5). A kinetic analysis revealed that both reactions proceeded according to pseudo-first-order kinetics, and their rate constants k_{fast}^{CTID} and k_{slow}^{CTID} were estimated to be 0.70 and 0.040 s^{−1}, respectively. Dioxetanes **2b** and **2c** similarly underwent dual-phase CTID.²² On the other hand, 4-hydroxyphenyl-analogue **3** decomposed simply according to pseudo-first-order kinetics to give blue light ($k^{CTID} = 0.14$ s^{−1}, $\lambda_{max}^{CL} = 471$ nm, $\Phi_{CL} = 1.1 \times 10^{-7}$) (Table 1, Figure 1).^{23,24} Such a simple single-phase decomposition has been recognized as a rather normal feature for most known CTID of dioxetanes such as furan-analogue **1**, for which rotational isomerism has hardly been observed.²

These facts suggested a formal feature that one rotamer (*syn* or *anti*) decomposed rapidly while the other decomposed slowly for the CTID of **2a**. However, it was not clear whether the rotamer with k_{slow}^{CTID} decomposed directly or first isomerized to another rotamer with k_{fast}^{CTID} and then decomposed: these two processes might occur concurrently. Thus, we carried out a preliminary control experiment as follows. The TBAF-induced decomposition of **2a** was quenched with trifluoroacetic acid after CTID with k_{fast}^{CTID} was almost completed. When TBAF was again added to this solution after an appropriate period, chemiluminescence due to the fast CTID was observed again (Supporting Information, Figure S6). This result showed that isomerization of the rotamer with k_{slow}^{CTID} into another with k_{fast}^{CTID} occurred during the TBAF-induced decomposition of **2a**, though direct decomposition of the former could not be denied.

Conclusion

The acylamino-substituted bicyclic dioxetanes **2**, **3**, and **4** designed and synthesized here were quite stable thermally and, in fact, showed higher thermal stability than most known dioxetanes. These dioxetanes were found to undergo base-induced chemiluminescent decomposition to give light with moderate to high efficiencies. In particular, dioxetane **4** underwent CTID with highly efficient chemiluminescence comparable to its oxy-analogue **26**. A notable characteristic of CTID for the present acylamino-substituted dioxetanes was that an *N*-acylamino-group influenced the color of the chemiluminescence and the rate of the decomposition k^{CTID} ,

(21) An MO calculation suggested that LUMO for an anion of **24** spread over imino moiety as well as an aromatic ring differently from that for an anion of **27**, which was localized on an aromatic ester (see the Supporting Information, Figure S4).

(22) Dioxetane **2d** underwent practically single-phase decomposition, though it also showed rotational isomerism as described previously. The rate of CTID was most likely far slower than *syn–anti* isomerization for **2d** (Table 1), so that the reaction was practically observed to proceed in a single phase. This was also the case for the CTID of **4**.

(23) The phenomenon in which CTID of a *p*-oxidophenyldioxetane gives light with shorter λ_{max}^{CL} and far lower Φ_{CL} than its meta-isomer for oxy-substituted dioxetanes such as **1** has been referred to as an “odd/even” relationship.^{6b,24}

(24) (a) McCapra, F. *Tetrahedron Lett.* **1993**, 34, 6941–6944. (b) Edwards, B.; Sparks, A.; Voyta, J. C.; Bronstein, I. *J. Org. Chem.* **1990**, 55, 6225–6229. (c) Matsumoto, M.; Hiroshima, T.; Chiba, S.; Isobe, R.; Watanabe, N.; Kobayashi, H. *Luminescence* **1999**, 14, 345–348. (d) Watanabe, W.; Kobayashi, H.; Azami, M.; Matsumoto, M. *Tetrahedron* **1999**, 55, 6831–6840. (e) Hoshiya, N.; Fukuda, N.; Watanabe, N.; Matsumoto, M. *Tetrahedron* **2006**, 62, 5808–5820.

and furthermore an *N*-acyl substituent could decisively affect the efficiency of singlet-chemiexcitation as observed for the case of **2b**.

Experimental Section

Singlet Oxygenation of *N*-Boc-4-*tert*-butyl-5-(3-hydroxyphenyl)-3,3-dimethyl-2,3-dihydropyrrole (5a). Typical Procedure. A solution of *N*-Boc-4-*tert*-butyl-5-(3-hydroxyphenyl)-3,3-dimethyl-2,3-dihydropyrrole (**5a**) (100 mg, 0.29 mmol) and tetraphenylporphyrin (TPP) (1 mg) in CH₂Cl₂ (10 mL) was irradiated externally with a 940 W Na lamp under an oxygen atmosphere at 0 °C for 40 min. After the photolysate was concentrated in vacuo, the residue was chromatographed on silica gel and eluted with ether–CH₂Cl₂ (1:4) to give 2-(Boc)-5-*tert*-butyl-1-(3-hydroxyphenyl)-4,4-dimethyl-2-aza-6,7-dioxabicyclo[3.2.0]heptane (**2a**) as a colorless solid (106 mg, 97% yield). Similarly, dihydropyrroles **5b–d**, **6**, and **7** were transformed to the corresponding dioxetanes **2b–d**, **3**, and **4** in respective yields of 85%, 92%, 87%, 93%, and 100%.

2a: colorless amorphous solid (55:45 mixture of conformational isomers); ¹H NMR (500 MHz, CDCl₃) δ_H 1.01 and 1.01 (s, 9H), 1.06–1.13 (m, 12H), 1.37 and 1.40 (s, 3H), 3.63 (d, *J* = 10.1 Hz, 1H), 4.06 and 4.07 (d, *J* = 10.1 Hz, 1H), 6.01 (1H × 0.45), 6.22 (broad s, 1H × 0.55), 6.78–6.88 (m, 2H), 7.15–7.27 (m, 2H) ppm; ¹³C NMR (125 MHz, CDCl₃) δ_C 20.6, 25.7 and 25.7, 27.3 and 27.3, 27.7 and 27.8, 37.8 and 37.9, 43.0 and 43.1, 62.9 and 63.0, 81.2 and 81.4, 104.7 and 104.8, 106.2 and 106.5, 114.0 and 116.2, 115.1 and 115.5, 119.3 and 121.1, 128.7 and 128.8, 139.3 and 139.4, 154.5 and 154.9, 155.7, and 155.8 ppm; IR (KBr) $\tilde{\nu}$ 3401, 2979, 2931, 1706, 1674, 1604, 1592 cm^{−1}; mass (*m/z*, %) 345 (M⁺ − 32, 0.3), 278 (29), 264 (14), 220 (62), 192 (23), 121 (100), 57 (46), 56 (20); HRMS (ESI) 400.2071, calcd for C₂₁H₃₁NO₅Na [M + Na⁺] 400.2100. Anal. Calcd for C₂₁H₃₁NO₅: C, 66.82; H, 8.28; N, 3.71. Found: C, 67.14; H, 8.50; N, 3.56.

2b: colorless needles, mp 159.5–160.0 °C dec (from CH₂Cl₂–hexane) (50:50 mixture of conformational isomers); ¹H NMR (400 MHz, CDCl₃) δ_H 1.00 and 1.01 (s, 9H), 1.13 (s, 3H), 1.48 and 1.52 (s, 3H), 3.84–4.04 (m, 1H), 4.19 and 4.20 (d, *J* = 10.5 Hz, 1H), 5.48 (broad s, 1H × 0.5), 5.95 (broad s, 1H × 0.5), 6.51 (d with fine coupling, *J* = 7.7 Hz, 1H × 0.5), 6.59 (d with fine coupling, *J* = 7.9 Hz, 1H × 0.5), 6.74 (s, 1H × 0.5), 6.83–7.09 (m, 1H), 6.87 (d, *J* = 7.6 Hz, 1H × 0.5), 7.05 (t, *J* = 7.9 Hz, 1H × 0.5), 7.13–7.40 (m, 5.5 H) ppm; ¹³C NMR (125 MHz, CDCl₃) δ_C 20.5 and 20.6, 25.7 and 25.7, 27.3, 37.9 and 38.0, 43.5 and 43.7, 64.0 and 64.1, 105.0 and 105.1, 106.0, and 106.2 (broad), 113.7 and 116.8, 115.6 and 115.9, 118.5 and 121.2, 127.4 and 127.5, 128.0 and 128.0, 128.8, 130.0, and 130.3 (broad), 136.2 and 136.4 (broad), 137.5 and 137.9, 155.6 and 155.7, 173.8, and 174.1 ppm; IR (KBr) $\tilde{\nu}$ 3310, 3006, 2980, 2965, 1650, 1622, 1599 cm^{−1}; mass (*m/z*, %) 381 (M⁺, 0.4), 349 (M⁺ − 32, 1), 278 (7), 204 (24), 176 (11), 122 (31), 121 (19), 105 (100), 77 (37), 57 (12); HRMS (ESI) 404.1859, calcd for C₂₃H₂₇NO₄Na [M + Na⁺] 404.1838. Anal. Calcd for C₂₃H₂₇NO₄·¹/₅CH₂Cl₂: C, 69.93; H, 6.93; N, 3.52. Found: C, 69.98; H, 7.14; N, 3.53.

2c: yellow plates, mp 146.0 °C dec (from CHCl₃–hexane) (50:50 mixture of conformational isomers); ¹H NMR (500 MHz, CDCl₃) δ_H 1.03 and 1.04 (s, 9H), 1.14 (s, 3H), 1.39 (s, 3H), 1.20–1.60 (m, 3H), 3.70–3.95 (m, 1H), 4.07 (d, *J* = 8.2 Hz, 1H), 6.76–6.91 (m, 2H), 7.16–7.32 (m, 2H) ppm; ¹³C NMR (125 MHz, CDCl₃) δ_C 20.8 and 20.9, 24.2 and 24.4, 25.9, 27.2 and 27.2, 37.9 and 37.9, 42.4 (broad), 63.5 and 63.6 (broad), 105.0 and 105.2, 106.9 (broad), 114.0 and 116.8, 116.2, 119.1 and 120.2, 129.4 and 129.5, 137.7 and 137.8, 156.8, 174.5 ppm; IR (KBr) $\tilde{\nu}$ 3366, 3014, 2965, 2939, 2884, 1642, 1603 cm^{−1}; mass (*m/z*, %) 319 (M⁺, 0.8), 287 (M⁺ − 32, 0.4), 262 (25), 234 (18), 220 (10), 121 (100), 93 (11), 57 (15); HRMS (ESI) 342.1668, calcd for C₁₈H₂₅NO₄Na

[M + Na⁺] 342.1681. Anal. Calcd for C₁₈H₂₅NO₄: C, 67.69; H, 7.89; N, 4.39. Found: C, 67.42; H, 8.07; N, 4.36.

2d: colorless amorphous solid (74:26 mixture of conformational isomers); ¹H NMR (500 MHz, CDCl₃) δ_H 0.97 (s, 9H × 0.74), 0.98 (s, 9H × 0.26), 1.15 (s, 3H × 0.26), 1.16 (s, 3H × 0.74), 1.44 (s, 3H × 0.26), 1.46 (s, 3H × 0.74), 1.40–1.63 (m, 6H), 3.21 (d, *J* = 9.2 Hz, 1H × 0.74), 3.27 (d, *J* = 9.2 Hz, 1H × 0.26), 3.25–3.45 (m, 4H), 4.11 (d, *J* = 9.2 Hz, 1H × 0.26), 4.14 (d, *J* = 9.2 Hz, 1H × 0.74), 6.41 (s, 1H × 0.26), 6.52 (dd, *J* = 8.0 and 2.1 Hz, 1H × 0.26), 6.65 (dd, *J* = 8.0 and 2.3 Hz, 1H × 0.74), 6.69 (d, *J* = 7.6 Hz, 1H × 0.74), 6.70 (s, 1H × 0.26), 6.80 (s, 1H × 0.74), 7.08 (dd, *J* = 8.0 and 7.6 Hz, 1H × 0.74), 7.14 (dd, *J* = 8.0 and 7.8 Hz, 1H × 0.26), 7.25 (s with fine coupling, 1H × 0.74), 7.45 (d, *J* = 7.8 Hz, 1H × 0.26) ppm; ¹³C NMR (125 MHz, CDCl₃) δ_C 20.1 and 20.1, 24.3, 25.1 and 25.2, 25.7 and 25.8, 27.0 and 27.1, 37.6, 44.1 and 44.3, 46.2 and 46.3, 62.7, 103.7 and 104.2, 105.4 and 105.6, 113.9 and 117.2, 115.6 and 115.8, 118.0 and 121.3, 128.4 and 128.6, 138.2 and 138.3, 156.0 and 156.4, 160.0, and 160.0 ppm; IR (KBr) $\tilde{\nu}$ 3360, 2938, 2862, 1680, 1641, 1592 cm^{−1}; mass (*m/z*, %) 388 (M⁺, 5), 331 (34), 303 (12), 278 (15), 247 (13), 121 (24), 112 (100), 84 (26), 69 (20), 57 (19); HRMS (ESI) 411.2216, calcd for C₂₂H₃₂N₂O₄Na [M + Na⁺] 411.2260. Anal. Calcd for C₂₂H₃₂N₂O₄·¹/₂₀CHCl₃: C, 67.14; H, 8.19; N, 7.10. Found: C, 67.49; H, 8.47; N, 7.11.

3: colorless plates, mp 143.0–143.5 °C dec (from CH₂Cl₂–hexane); ¹H NMR (400 MHz, CDCl₃) δ_H 0.98 (s, 9H), 1.10 (s, 9H), 1.11 (s, 3H), 1.38 (s, 3H), 3.59 (d, *J* = 9.9 Hz, 1H), 4.04 (d, *J* = 9.9 Hz, 1H), 5.11 (s, 1H), 6.77–6.82 (m, 2H), 7.15–7.20 (m, 1H), 7.51–7.55 (m, 1H) ppm; ¹³C NMR (125 MHz, CDCl₃) δ_C 20.6, 25.7, 27.2, 27.8, 37.7, 42.9, 62.8, 81.2, 105.1, 105.7, 114.4, 114.9, 128.5, 129.3, 129.8, 154.9, 156.3 ppm; IR (KBr) $\tilde{\nu}$ 3272, 2979, 2893, 1701, 1666, 1616, 1594 cm^{−1}; mass (*m/z*, %) 377 (M⁺, trace), 345 (M⁺ − 32, 2), 220 (29), 121 (100), 57 (39), 56 (28); HRMS (ESI) 400.2089, calcd for C₂₁H₃₁NO₅Na [M + Na⁺] 400.2100. Anal. Calcd for C₂₁H₃₁NO₅·¹/₁₀H₂O: C, 66.50; H, 8.29; N, 3.69. Found: C, 66.32; H, 8.41; N, 3.68.

4: Colorless plates, mp 160.5–161.0 °C dec (from CH₂Cl₂–hexane) (52:48 mixture of conformational isomers); ¹H NMR (400 MHz, CDCl₃) δ_H 1.05 and 1.06 (s, 9H), 1.11 (s, 3H), 1.14 (s, 9H), 1.42 and 1.45 (s, 3H), 3.63 (d, *J* = 10.0 Hz, 1H), 4.08 and 4.09 (d, *J* = 10.0 Hz, 1H), 6.94 (dd, *J* = 8.3 and 1.7 Hz, 1H × 0.48), 7.10 (d, *J* = 1.7 Hz, 1H × 0.52), 7.35 (dd, *J* = 8.3 and 1.7 Hz, 1H × 0.52), 7.39–7.55 (m, 2H), 7.48 (d, *J* = 1.7 Hz, 1H × 0.48), 7.64 (d, *J* = 8.3 Hz, 1H × 0.48), 7.72 (d, *J* = 8.3 Hz, 1H × 0.52), 7.88–7.94 (m, 1H), 7.99 (d, *J* = 8.3 Hz, 1H), 12.53 (broad s, 1H) ppm; ¹³C NMR (125 MHz, CDCl₃) δ_C 20.6 and 20.6, 25.7 and 25.8, 27.3 and 27.4, 27.8 and 27.9, 37.9 and 38.0, 43.1 and 43.2, 62.9 and 63.0, 81.2 and 81.2, 104.1 and 104.3, 106.5, 116.0 and 116.6, 116.6 and 120.1, 118.6 and 118.9, 121.5 and 121.5, 122.2, 125.7 and 125.7, 126.8 and 126.8, 127.2 and 127.6, 132.5 and 132.6, 142.9 and 142.9, 151.7 and 151.8, 154.1 and 154.2, 157.2 and 157.6, 168.6, and 168.8 ppm; IR (KBr) $\tilde{\nu}$ 3417, 2978, 2930, 1717, 1630 cm^{−1}; mass (*m/z*, %) 510 (M⁺, 5), 410 (20), 354 (16), 353 (60), 326 (12), 325 (30), 283 (17), 270 (20), 255 (17), 254 (100), 226 (26), 198 (29), 197 (11), 57 (33), 56 (22); HRMS (ESI) 511.2280, calcd for C₂₈H₃₅N₂O₅S [M + H⁺] 511.2267, 533.2084, calcd for C₂₈H₃₄N₂O₅Na [M + Na⁺] 533.2086. Anal. Calcd for C₂₈H₃₄N₂O₅S: C, 65.86; H, 6.71; N, 5.49. Found: C, 65.52; H, 6.73; N, 5.33.

Base-Induced Decomposition of 2-Boc-5-*tert*-butyl-1-(3-hydroxyphenyl)-4,4-dimethyl-2-aza-6,7-dioxabicyclo[3.2.0]heptane (2a). Typical Procedure. A solution of 2-Boc-5-*tert*-butyl-1-(3-hydroxyphenyl)-4,4-dimethyl-2-aza-6,7-dioxabicyclo[3.2.0]heptane (**2a**) (50.0 mg, 0.13 mmol) in dry DMSO (1 mL) was added dropwise over 2 min to a solution of TBAF (1 mL/L in THF) (0.65 mL, 0.65 mmol) in dry DMSO (1 mL) under a nitrogen atmosphere at room temperature then the mixture was stirred for 15 min. The reaction mixture was poured into sat. aq. NH₄Cl and then extracted with AcOEt. The aqueous layer was

extracted again with AcOEt. The combined organic layer was washed twice with sat. aq NaCl, dried over MgSO₄, and concentrated in vacuo. The residue was chromatographed on silica gel and eluted with hexane–AcOEt (9:1) to give *N*-Boc-*N*-(2,2,4,4-tetramethyl-3-oxopentyl) 3-hydroxybenzamide (**22a**) as a colorless oil (46.5 mg, 93% yield).

Dioxetanes **2b–d**, **3**, and **4** were similarly decomposed by treatment with TBAF/DMSO system to give keto imides **22b–d**, **23**, and **24** in 99%, 89%, 97%, 94%, and 99% yield.

22a: colorless oil; ¹H NMR (500 MHz, CDCl₃) δ_H 1.10 (s, 9H), 1.33 (s, 9H), 1.34 (s, 6H), 4.06 (s, 2H), 6.98 (d with fine coupling, *J* = 7.8 Hz, 1H), 7.16–7.20 (m, 2H), 7.24 (t, *J* = 7.8 Hz, 1H), 7.20–7.30 (m, 1H) ppm; ¹³C NMR (125 MHz, CDCl₃) δ_C 25.0, 27.2, 28.2, 46.3, 51.0, 52.6, 83.2, 114.8, 118.5, 119.7, 129.4, 138.9, 153.9, 156.0, 173.8, 217.7 ppm; IR (liquid film) ν̄ 3403, 2978, 2930, 1732, 1677, 1599 cm^{−1}; mass (*m/z*, %) 320 (M⁺ − 57, 10), 264 (20), 236 (11), 221 (11), 220 (68), 192 (24), 163 (11), 121 (100), 57 (44); HRMS (ESI) 400.2065, calcd for C₂₁H₃₁NO₅Na [M + Na⁺] 400.2100.

22b: colorless oil; ¹H NMR (500 MHz, CDCl₃) δ_H 1.39 (s, 9H), 1.41 (s, 6H), 4.30 (s, 2H), 6.65–6.71 (m, 1H), 6.91–7.02 (m, 4H), 7.10 (dd, *J* = 7.8 and 7.3 Hz, 2H), 7.20 (t, *J* = 7.8 Hz, 1H), 7.38 (d with fine coupling, *J* = 7.3 Hz, 2H) ppm; ¹³C NMR (125 MHz, CDCl₃) δ_C 25.5, 28.2, 46.4, 51.5, 54.8, 115.8, 119.2, 121.1, 128.1, 128.8, 129.6, 131.6, 136.6, 137.8, 155.8, 174.5, 174.7, 217.6 ppm; IR (liquid film) ν̄ 3388, 2973, 2930, 2873, 1699, 1679, 1657, 1598 cm^{−1}; mass (*m/z*, %) 381 (M⁺, 1), 324 (35), 296 (31), 122 (16), 121 (80), 105 (100), 77 (20), 57 (14); HRMS (ESI) 404.1835, calcd for C₂₃H₂₇NO₄Na [M + Na⁺] 404.1838.

22c: colorless oil; ¹H NMR (500 MHz, CDCl₃) δ_H 1.27 (s, 9H), 1.31 (s, 6H), 2.01 (s, 3H), 4.08 (s, 2H), 7.08 (d, *J* = 7.8 Hz, 1H), 7.28 (s with fine coupling, 1H), 7.31 (dd, *J* = 7.8 and 1.4 Hz, 1H), 7.34 (t, *J* = 7.8 Hz, 1H), 7.64 (broad s, 1H) ppm; ¹³C NMR (125 MHz, CDCl₃) δ_C 24.9, 25.8, 28.0, 46.1, 51.0, 53.6, 115.9, 120.7, 121.3, 130.3, 136.3, 156.7, 173.1, 175.0, 217.7 ppm; IR (liquid film) ν̄ 3361, 3055, 2983, 1704, 1666, 1599 cm^{−1}; mass (*m/z*, %) 319 (M⁺, 1), 262 (26), 234 (17), 220 (10), 121 (100), 93 (11), 57 (17); HRMS (ESI) 342.1645, calcd for C₁₈H₂₅NO₄Na [M + Na⁺] 342.1681.

22d: colorless oil; ¹H NMR (500 MHz, CDCl₃) δ_H 1.30 (s, 9H), 1.37 (s, 6H), 0.90–1.65 (m, 6H), 2.50–3.57 (m, 4H), 4.05 (s, 2H), 6.93 (dd, *J* = 8.0 and 2.3 Hz, 1H), 7.07 (d, *J* = 7.6 Hz, 1H), 7.13 (s with fine coupling, 1H), 7.20 (dd, *J* = 8.0 and 7.6 Hz, 1H), 7.99 (s, 1H) ppm; ¹³C NMR (125 MHz, CDCl₃) δ_C 23.7, 24.6 (broad), 28.4, 45.2 (broad), 46.0, 47.6 (broad), 50.8, 54.4, 114.5, 118.8, 119.3, 129.4, 136.2, 156.5, 157.0, 170.5, 217.1 ppm; IR (liquid film) ν̄ 3331, 3055, 2984, 2947, 2862, 1679, 1642, 1597 cm^{−1}; mass (*m/z*, %) 388 (M⁺, 8), 332 (18), 331 (73), 303 (25), 247 (23), 121 (23), 112 (100), 84 (11); HRMS (ESI) 411.2258, calcd for C₂₂H₃₂N₂O₄Na [M + Na⁺] 411.2260.

23: colorless viscous oil; ¹H NMR (500 MHz, CDCl₃) δ_H 1.16 (s, 9H), 1.33 (s, 9H), 1.35 (s, 6H), 4.08 (s, 2H), 6.77 (d with fine coupling, *J* = 8.4 Hz, 2H), 7.57 (d with fine coupling, *J* = 8.4 Hz, 2H), 7.67 (broad s, 1H) ppm; ¹³C NMR (125 MHz, CDCl₃) δ_C 24.9, 27.4, 28.2, 46.3, 51.0, 52.7, 82.9, 115.0, 128.8, 130.7, 154.3, 159.9, 173.7, 218.5 ppm; IR (liquid film) ν̄ 3387, 2978, 2933, 1726, 1674, 1607 cm^{−1}; mass (*m/z*, %) 377 (M⁺, trace), 220 (39), 121 (100), 57 (22); HRMS (ESI) 400.2052, calcd for C₂₁H₃₁NO₅Na [M + Na⁺] 400.2100.

24: colorless plates, mp 162.0–164.0 °C (from CH₂Cl₂–hexane); ¹H NMR (500 MHz, CDCl₃) δ_H 1.17 (s, 9H), 1.32

(s, 9H), 1.37 (s, 6H), 4.09 (s, 2H), 7.26 (dd, *J* = 8.2 and 1.8 Hz, 1H), 7.33 (d, *J* = 1.8 Hz, 1H), 7.44 (dd, *J* = 7.8 and 7.3 Hz, 1H), 7.53 (dd, *J* = 7.8 and 7.3 Hz, 1H), 7.74 (d, *J* = 8.2 Hz, 1H), 7.92 (d, *J* = 7.8 Hz, 1H), 8.00 (d, *J* = 7.8 Hz, 1H) ppm; ¹³C NMR (125 MHz, CDCl₃) δ_C 25.0, 27.4, 28.2, 46.1, 50.7, 52.4, 83.5, 117.1, 118.5, 118.7, 121.6, 122.4, 126.0, 126.9, 128.0, 132.8, 141.6, 151.7, 153.6, 157.6, 168.3, 172.5, 216.3 ppm; IR (KBr) ν̄ 2983, 2932, 1733, 1684, 1669, 1566 cm^{−1}; mass (*m/z*, %) 510 (M⁺, 10), 410 (22), 397 (14), 354 (23), 353 (82), 326 (14), 325 (36), 296 (13), 283 (21), 270 (18), 255 (18), 254 (100), 226 (22), 198 (23), 57 (29); HRMS (ESI) 511.2295, calcd for C₂₈H₃₅N₂O₅S [M + H⁺] 511.2267. Anal. Calcd for C₂₈H₃₄N₂O₅S · 2.5H₂O: C, 60.52; H, 7.07; N, 5.04. Found: C, 60.40; H, 6.68; N, 5.24.

Time Course for the Thermal Decomposition of Dioxetanes 2a,b. General Procedure. A solution of dioxetane **2a,b** (3–5 mg) in *p*-xylene-*d*₁₀ (0.8 mL) in a ¹H NMR sample tube was heated by means of a liquid paraffin bath thermostated at an appropriate temperature of 90–110 °C. After being heated at regular intervals, the samples were subjected to ¹H NMR analysis to determine the ratio of intact **2a,b** to the corresponding keto imide **22a,b**.

Chemiluminescence Measurement and Time Course for the Charge-Transfer-Induced Decomposition of Dioxetanes. General Procedure. Chemiluminescence was measured with a JASCO, FP-750, a FP-6500 spectrometer, and/or a Hamamatsu Photonics PMA-11 multichannel detector.

A freshly prepared solution (2.0 mL) of TBAF (1.0 × 10^{−2} mol dm^{−3}) in DMSO was transferred to a quartz cell (10 × 10 × 50 mm³) and the latter was placed in the spectrometer, which was thermostated with stirring at 25 °C. After 3–5 min, a solution of the dioxetane **2a,b**, **3**, or **4** in DMSO (1.0 × 10^{−5} mol dm^{−3}, 1.0 mL) was added by means of a syringe and measurement was started immediately. The time-course of the intensity of light emission was recorded and processed according to first-order kinetics. The total light emission was estimated by comparing it to that of an adamantylidene-dioxetane, the chemiluminescence efficiency Φ^{CL} of which has been reported to be 0.29 and which was used here as a standard.^{19,20}

Fluorescence Measurement of Authentic Emitters 25a–d and Oxido Anion of 24. A freshly prepared solution of 2.00–2.10 × 10^{−5} mol dm^{−3} of **22a–d** or **24**, and of 1.0 × 10^{−2} mol dm^{−3} of TBAF in DMSO was transferred to a quartz cell (10 × 10 × 50 mm³) and the latter placed in the spectrometer, which was thermostated with stirring at 25 °C. Thus, the fluorescence spectra of **25a–d** and oxido anion of **24** were measured and their fluorescence efficiencies (Φ^{fl}) were estimated with fluorescein as a standard.

Acknowledgment. We gratefully acknowledge financial assistance provided by Grants-in-aid (No. 17550050 and No. 21550052) for Scientific Research from the Ministry of Education, Culture, Sports, Science, and Technology, Japan.

Supporting Information Available: General method for the Experimental Section, ¹H NMR/¹³C NMR spectra of **2a–d**, **3**, **4**, **5a–d**, **6**, **7**, **8a–d**, **9**, **10**, **11**, **13**, **14a–d**, **15**, **17**, **18**, **20**, **21**, **22a–d**, **23**, and **24**, and ORTEP views and CIFs for **4** and **14a-trans**. This material is available free of charge via the Internet at <http://pubs.acs.org>.